

Observation of momentum space semi-localization in Si-doped β -Ga₂O₃

Cite as: Appl. Phys. Lett. **101**, 232105 (2012); <https://doi.org/10.1063/1.4769109>

Submitted: 27 July 2012 • Accepted: 13 November 2012 • Published Online: 04 December 2012

P. Richard, T. Sato, S. Souma, et al.



View Online



Export Citation



CrossMark

ARTICLES YOU MAY BE INTERESTED IN

[A review of Ga₂O₃ materials, processing, and devices](#)

Applied Physics Reviews **5**, 011301 (2018); <https://doi.org/10.1063/1.5006941>

[Oxygen vacancies and donor impurities in \$\beta\$ -Ga₂O₃](#)

Applied Physics Letters **97**, 142106 (2010); <https://doi.org/10.1063/1.3499306>

[Recent progress on the electronic structure, defect, and doping properties of Ga₂O₃](#)

APL Materials **8**, 020906 (2020); <https://doi.org/10.1063/1.5142999>

 QBLOX



1 qubit

Shorten Setup Time

Auto-Calibration
More Qubits

Fully-integrated

Quantum Control Stacks
Ultrastable DC to 18.5 GHz
Synchronized <<1 ns
Ultralow noise



100s qubits

[visit our website >](#)

Observation of momentum space semi-localization in Si-doped β -Ga₂O₃

P. Richard,^{1,a)} T. Sato,² S. Souma,³ K. Nakayama,² H. W. Liu,¹ K. Iwaya,³ T. Hitosugi,³
 H. Aida,⁴ H. Ding,¹ and T. Takahashi^{2,3}

¹Beijing National Laboratory for Condensed Matter Physics and Institute of Physics,
 Chinese Academy of Sciences, Beijing 100190, China

²Department of Physics, Tohoku University, Sendai 980-8578, Japan

³WPI Research Center, Advanced Institute for Materials Research, Tohoku University,
 Sendai 980-8577, Japan

⁴Namiki Precision Jewel Co., Ltd., Tokyo 123-8511, Japan

(Received 27 July 2012; accepted 13 November 2012; published online 4 December 2012)

We performed an angle-resolved photoemission spectroscopy study of Si-doped β -Ga₂O₃. We observed very small photoemission intensity near the Fermi level corresponding to non-dispersive states assigned to Si impurities. We show evidence for a quantization of these states that is accompanied by a confinement in the momentum space consistent with a real-space finite confinement observed in a previous scanning tunneling microscopy study. Our results suggest that this semi-localization in the conjugate spaces plays a crucial role in the electronic conduction of this material. © 2012 American Institute of Physics. [<http://dx.doi.org/10.1063/1.4769109>]

Its transparency and relatively high conductivity compared to other semiconductors, even at low temperature (T), promote the wide gap semiconductor β -Ga₂O₃ as an attractive candidate for optoelectronic applications.¹ Despite general enthusiasm for this material, there is no commonly accepted picture to explain its conductivity, which calls for a complete characterization of the electronic states near the Fermi level (E_F) of this material. A recent scanning tunneling microscopy (STM) investigation of Si-doped β -Ga₂O₃ evidenced the presence of Si impurity donor states very near E_F .² From their spatial extension Δr , the authors conjectured that conductivity likely occurs from hopping between nearby impurities. However, STM is a real (r) space measurement that cannot image directly how electrons propagate in materials. As a natural complement, angle-resolved photoemission spectroscopy (ARPES) is a powerful tool to access directly the electronic band structure of materials in the momentum (k) space that can be used to address this problem. Unfortunately, previous ARPES studies of β -Ga₂O₃ did not report any state near E_F .^{3,4}

Here, we report an ARPES characterization of the electronic states at low-energy (E) in the k space of Si-doped β -Ga₂O₃. We observe very weak intensity signal at the Brillouin zone (BZ) center associated to non-dispersive states likely related to Si impurities. We show that these states are quantized and that their corresponding momentum distribution curve (MDC) profiles remain restricted in k space over a wide E range.

Single crystals of β -Ga₂O₃ were grown using an edge-defined film-fed growth method and electron-doped to a concentration of $\sim 1 \times 10^{-19} \text{ cm}^{-3}$ with Si atoms.⁵ ARPES measurements were performed with photon energy ($h\nu$) in the 20–200 eV range at the U1-NIM and Apple-PGM beamlines of the Synchrotron Radiation Center (Stoughton, WI) using a VG-Scienta R4000 and a VG-Scienta SES 2002 multichannel analyzers, respectively. Additional measurements

were performed in Tohoku University using a VG-Scienta SES 2002 multichannel analyzer and the He-I α line of a He-discharging lamp ($h\nu = 21.218 \text{ eV}$). The samples were cleaved *in situ* along the (100) plane and maintained in a vacuum better than 10^{-10} Torr. A previous STM study on samples from the same batch indicates that the cleaved samples have atomically flat surfaces.² We systematically checked that the samples were not charged by varying the intensity of the incident light beam.

We show in Fig. 1(a) a typical core level spectrum of β -Ga₂O₃ recorded with $h\nu = 195 \text{ eV}$. In addition to excitations at -146.5 eV and -143 eV attributed to Auger transitions from their $h\nu$ dependence (kinetic energies E_K of 44.0 and 47.5 eV, respectively), most of the peaks can be simply assigned to Ga and O core levels. The spectrum is dominated by the weakly dispersive Ga 3d states at a binding energy (E_B) of 21.66 eV. In comparison, the intensity of the valence band originating from O 2p states is one order of magnitude weaker. It locates between 4.6 and 13 eV (tail to tail) below E_F . As expected from the 4.5–4.9 eV semiconducting gap reported for this material,^{1,6–8} the spectral intensity is almost 0 up to E_F . Nevertheless, the near- E_F zoom displayed in inset indicates a finite density of states, with a spectral intensity 10^3 times smaller than that of the valence band at this particular $h\nu$ value.

This small density of states at E_F was not detected in previous ARPES studies focusing on the valence band and the semiconducting gap.^{3,4} To characterize it further, we performed careful ARPES measurements near E_F . Band structure calculations⁹ predict a minimum at the BZ center (Γ) for the conduction band of β -Ga₂O₃. Accordingly, the FS displayed in Fig. 1(b) shows only a very small spot of intensity at Γ . However, the energy distribution curves (EDCs) corresponding to an ARPES cut crossing the Γ point given in Fig. 1(c) do not show evidence for dispersion within our experimental accuracy. The spectrum recorded exactly at Γ shows a 2-peak feature that will be described below. The spectral intensity fades rapidly away from Γ and is already

^{a)}Electronic address: p.richard@iphy.ac.cn.

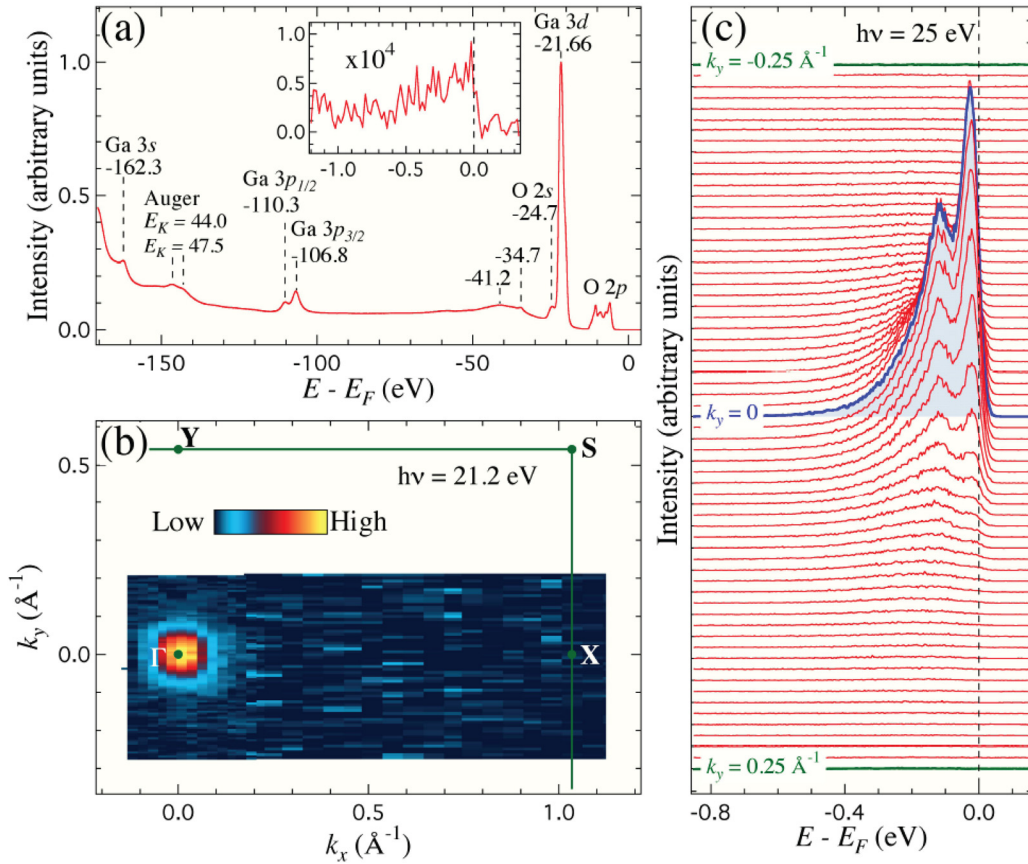


FIG. 1. (a) Photoemission spectra of β -Ga₂O₃ recorded with $h\nu = 195$ eV. Inset: 10^4 zoom near E_F . (b) FS intensity map. (c) EDCs recorded around Γ with $h\nu = 25$ eV.

virtually zero at $k_y = \pm 0.25 \text{ \AA}^{-1}$, where no Fermi edge is detected.

The relationship between k_z and the $h\nu$ allows us to estimate the electronic dispersion along this direction.¹⁰ Such procedure has been performed previously for the valence band of β -Ga₂O₃.³ To investigate the k_z variations of the near- E_F states, we performed $h\nu$ dependent measurements over a wide E range. We show in Figs. 2(a)–2(i) ARPES intensity cuts recorded with $h\nu$ between 20 eV and 28 eV. With $h\nu$ increasing from 20 eV, the spectral intensity increases and reaches a maximum at 26 eV, before it starts to decrease. Although the intensity of the ARPES spectra depends on $h\nu$, the spectral shape seems not to vary significantly. In particular, the 2-peak structure is well observed at each $h\nu$ value. This assertion is confirmed by the EDCs at the Γ point, which are shown in Fig. 2(j). Despite strong intensity variation, the lineshape of the EDCs and the position of the two peaks are quite constant. This indicates that the states do not disperse along k_z , in contrast to band structure calculations suggesting that the bottom of the conduction band at Γ is highly dispersive along k_z .⁹ As we show in Fig. 2(k), we find a resonance at 26 eV that we can assign univocally to neither Ga nor Si electronic states.

Additional information on the near- E_F states can be obtained by varying the polarization of the incident photons. In Fig. 3, we compare spectra at the Γ point obtained with π and σ polarized photons. Unlike the π polarization, the σ polarization is not pure in our experiment and the corresponding vector potential has a finite component perpendicular to

the surface. Indeed, this component is mainly responsible for the differences in the EDCs displayed in Fig. 3(a) since they are recorded at normal emission and thus they should be identical for pure π and σ configurations. As confirmed with the ARPES intensity plots shown in Figs. 3(b) and 3(c), polarization strongly modulates the spectral intensity. This is also true for the near- E_F states, as indicated by the near- E_F ARPES intensity plots given in Figs. 3(d) and 3(e) for σ and π polarizations, respectively. The strong loss of spectral intensity in the π configuration as compared to the σ configuration, even for the normal emission EDCs shown in the inset of Fig. 3(a), strongly suggests that the states near- E_F are associated with z -oriented orbitals. Due to the absence of k dispersion, the states observed are most likely related with the $3p_z$ orbitals of the Si donors. However, our experiments do not allow us to completely rule out alternative scenarios such as a surface state related to the conduction band. In this latter case though, one would expect clear in-plane dispersion, which differs from our observation.

Our previous assignment is somewhat unconventional since an object localized in the r space, such as a Si dopant atom, should lead to electronic states completely delocalized in k space, which contrasts with our observation of ARPES intensity uniquely in the vicinity of the BZ center. To solve this apparent dilemma, we proceed in two steps. We first turn our attention to the lineshape associated with the near- E_F states. For this purpose, we performed measurements at lower T (10 K) and took advantage of the higher E resolution provided by a He-discharge lamp. The resulting ARPES

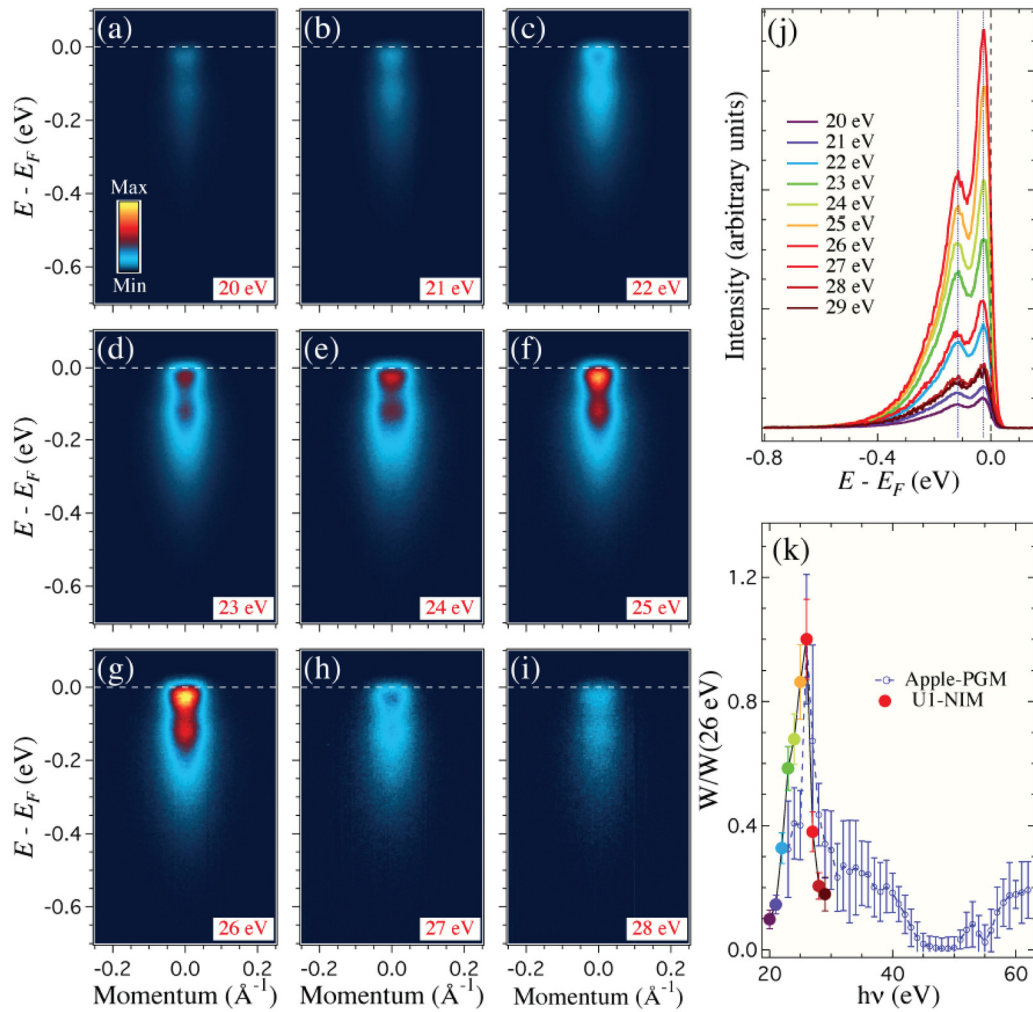


FIG. 2. (a)-(i) $h\nu$ dependence of an ARPES cut crossing the Γ point. (j) $h\nu$ dependence of the EDC at the Γ point recorded at the UI-NIM beamline of the Synchrotron Radiation Center. The blue dotted lines are guides for the eye. (k) $h\nu$ dependence of the spectral weight W integrated between -0.6 and 0.1 eV and normalized at $h\nu = 26$ eV. The color code for the data recorded at the UI-NIM beamline (full symbols) is the same as in panel (j).

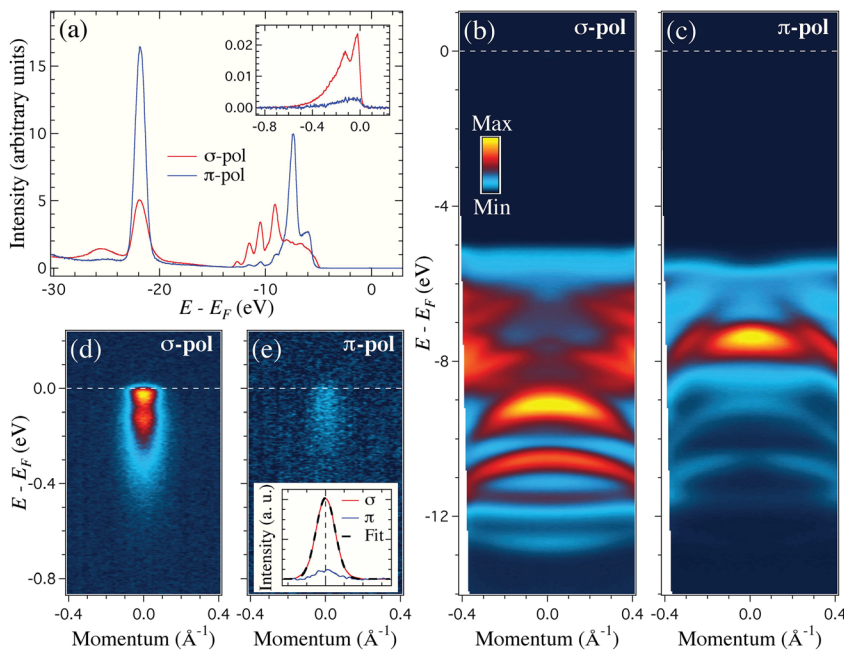


FIG. 3. (a) Comparison of EDCs at the Γ point recorded using $h\nu = 62$ eV with π and σ polarizations. An Al filter was used to suppress the strong second order light background. Inset: near- E_F zoom. (b) ARPES intensity plot near Γ recorded with 62 eV σ -polarized photons. (c) Same as (b) but using π -polarized photons. (d) Near- E_F zoom of the ARPES intensity plot in (b). (e) Near- E_F zoom of the ARPES intensity plot in (c). Inset: MDCs corresponding to data in (d) and (e), integrated from $E_B = 170$ meV up to E_F . The MDC recorded with σ -polarized light is perfectly fit with a gaussian distribution.

intensity plot is displayed in Fig. 4(a). The two peaks observed in the synchrotron data are still observed at 18 ± 3 meV and 120 ± 9 meV below E_F . In addition, the corresponding curvature intensity plot¹¹ shown in Fig. 4(b) reveals a third feature at 220 ± 20 meV that is confirmed by a broad shoulder in the integrated EDC displayed in the inset of the same panel. Although it cannot be resolved within the current experiment, the tail of the EDC extends to relatively high E_B , suggesting the possible presence of additional peaks. As far as our measurements allow us to resolve them, the three peaks observed are evenly spaced by $\Delta \simeq 100$ meV. Noteworthy, we found experimentally that Δ varies up to 10% from one sample to another, suggesting a possible relationship with Si doping or with the precise distribution of the Si impurities.

What can cause such a quantization of the electronic states? One may naively propose that a bosonic mode of energy Δ interacts with the electronic structure. Indeed, Raman studies of β -Ga₂O₃ report several phonon modes for energies slightly smaller than 100 meV.^{12–14} However, such interaction usually leads to an anomaly or “kink” in the electronic band dispersion observed by ARPES due to the opening of an energy gap. For example, this situation is often found in the superconducting state of copper-based^{15,16} and iron-based¹⁷ high-temperature superconductors. A more likely scenario is the presence of a quantum well (QW).¹⁸

Actually, a QW has already been proposed to explain the optical absorption spectra of minority acceptor states in the vicinity of the valence band.¹⁹ An important corollary to the presence of a QW associated with the electronic states of the Si impurities is that these electronic states are confined only within a typical distance Δr . The Heisenberg uncertainty principle thus implies that the same states are confined in k space as well within a momentum Δk of the order of $1/\Delta r$.

To investigate this scenario, we analyze the MDC profile of the near- E_F states. In the inset of Fig. 3(c), we compare the MDCs at E_F recorded on the same sample using σ and π polarizations. Except for an intensity difference, both profiles are similar and can be fit perfectly with a gaussian function. Noteworthy, such behavior is similar to first principle calculations on oxygen-vacancy-disordered ZnO predicting k space semi-localization for the O vacancy impurity states,²⁰ characterized by a loss of spectral coherence away from the zone center. Interestingly, gaussian functions can be used in β -Ga₂O₃ to fit the MDCs down to at least 500 meV below E_F , which is way below the 3 impurity levels identified by ARPES but still inside the tail of the near- E_F feature. In Fig. 4(c), we show the E dependence of the half-width at half-maximum (HWHM) corresponding to the fits obtained for various $h\nu$ values. Except for the low E part where small anomalies are observed, the HWHM increases linearly with E_B but remains finite, and no obvious influence

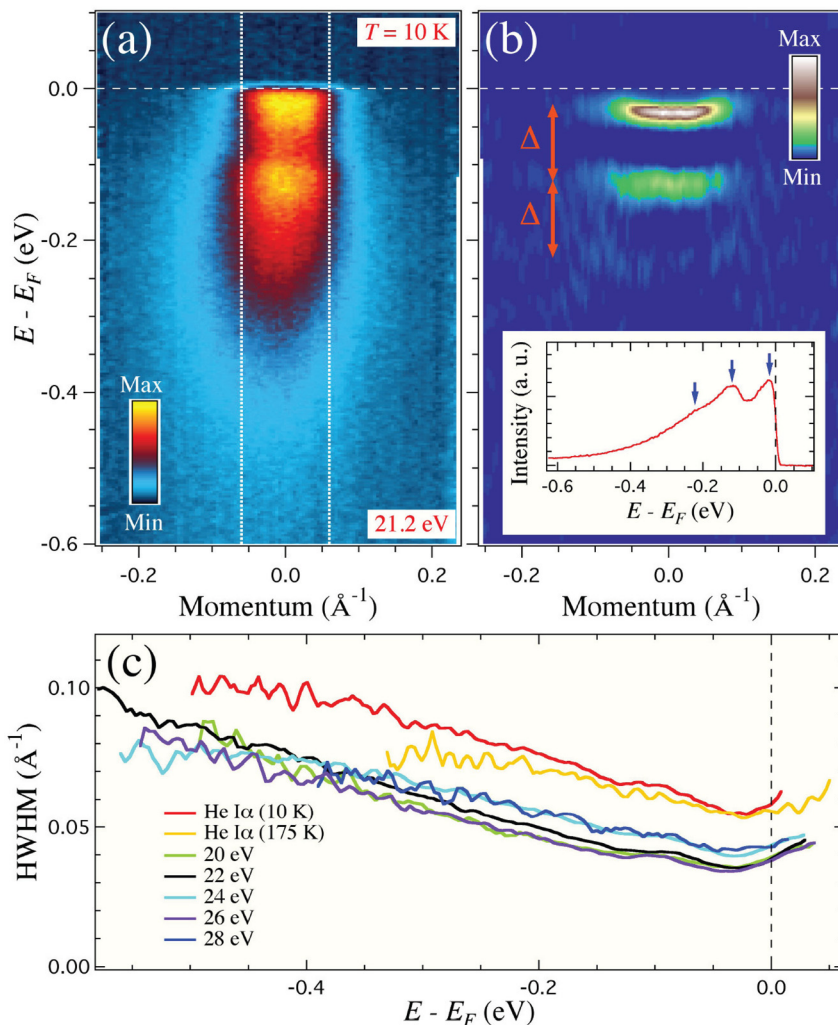


FIG. 4. (a) ARPES intensity plot recorded at 10 K with the He I α line. (b) Corresponding curvature intensity plot.¹¹ Inset: EDC integrated between the vertical white dotted lines in (a). Blue arrows indicate the position of the electronic states. (c) HWHM of the MDCs as a function of E_B for different $h\nu$ values. The results are from the same measurement, except for data obtained with the He discharged lamp (21.218 eV). The synchrotron data have been obtained at 50 K while the He lamp data were recorded at 10 K and 175 K.

from the probing $h\nu$ is noticed. Near E_F , the HWHM is about $0.040 \pm 0.005 \text{ \AA}^{-1}$ for the synchrotron data presented in Fig. 3(c). As with the QW spacing, the HWHM varies slightly from sample to sample. For example, the high- E resolution data shown in Fig. 3(a) are associated with a low- T HWHM of $0.055 \pm 0.005 \text{ \AA}^{-1}$, value that is quite robust against T .

By rounding up the HWHM to 0.05 \AA^{-1} and associating this value to Δk , we find that the corresponding spatial extension of the impurity wave function is about 20 \AA . This value is quite consistent with a previous STM study on samples from the same batch.² Indeed, the “size” of the impurities can be characterized by a decay length in the spectral intensity at a bias voltage corresponding to the donor states. Values ranging from 6 to 24 \AA were found for Si impurities in different locations.² Our ARPES results confirm that these states carry some k information, more precisely on the k distribution of the spectral coherence. As a consequence, they can promote electrical conduction for Si concentration sufficiently high to allow the wave functions from different impurities to percolate.

We caution that our interpretation of the multiple E levels in terms of a QW is not unique. Indeed, the conduction band is expected to locate in the same E range and could potentially explain some of the spectral intensity. Yet, the absence of obvious k dispersion remains puzzling and further theoretical and experimental studies are necessary to solve this issue. Nevertheless, our observation of a characteristic length for the k -space confinement of the spectral intensity is well supported and is a step towards a better understanding of the electronic properties of $\beta\text{-Ga}_2\text{O}_3$.

We are grateful to J.-P. Hu, W. Ku, and X. Dai for useful discussions. This work was supported by the Chinese Academy of Sciences (Grant No. 2010Y1JB6), the Ministry of Science and Technology of China (Grant Nos. 2010CB923000 and 2011CBA0010), the Nature Science Foundation of China (Grant Nos. 10974175, 11004232, and 11050110422), the Japan Society for the Promotion of Sciences, and MEXT of Japan. This work was based in part upon research conducted

at the Synchrotron Radiation Center which was primarily funded by the University of Wisconsin-Madison with supplemental support from facility Users and the University of Wisconsin-Milwaukee.

- ¹N. Ueda, H. Hosono, R. Waseda, and H. Kawazoe, *Appl. Phys. Lett.* **71**, 933 (1997).
- ²K. Iwaya, R. Shimizu, H. Aida, T. Hashizume, and T. Hitosugi, *Appl. Phys. Lett.* **98**, 142116 (2011).
- ³T. C. Lovejoy, E. N. Yitamben, N. Shamir, J. Morales, E. G. Villora, K. Shimamura, S. Zheng, F. S. Ohuchi, and M. A. Olmstead, *Appl. Phys. Lett.* **94**, 081906 (2009).
- ⁴C. Janowitz, V. Scherer, M. Mohamed, A. Krapf, H. Dwelk, R. Manzke, Z. Galazka, R. Uecker, K. Irmischer, R. Fornari, M. Michling, D. Schmeisser, J. R. Weber, J. B. Varley, and C. G. Van de Walle, *New J. Phys.* **13**, 085014 (2011).
- ⁵H. Aida, K. Nishiguchi, H. Takeda, N. Aota, K. Sunakawa, and Y. Yaguchi, *Jpn. J. Appl. Phys., Part 1* **47**, 8506 (2008).
- ⁶H. H. Tippins, *Phys. Rev.* **140**, A316 (1965).
- ⁷G. Blasse and A. Baril, *J. Phys. Chem. Solids* **31**, 707 (1970).
- ⁸T. Matsumoto, M. Aoki, A. Kinoshita, and T. Aono, *Jpn. J. Appl. Phys., Part 1* **13**, 1578 (1974).
- ⁹H. He, R. Orlando, M. A. Blanco, and R. Pandey, *Phys. Rev. B* **74**, 195123 (2006).
- ¹⁰A. Damascelli, *Phys. Scr., T* **109**, 61 (2004).
- ¹¹P. Zhang, P. Richard, T. Qian, Y.-M. Xu, X. Dai, and H. Ding, *Rev. Sci. Instrum.* **82**, 043712 (2011).
- ¹²Y. H. Gao, Y. Bando, T. Sato, Y. F. Zhang, and X. Q. Gao, *Appl. Phys. Lett.* **81**, 2267 (2002).
- ¹³R. Rao, A. M. Rao, B. Xu, J. Dong, S. Sharma, and M. K. Sunkara, *J. Appl. Phys.* **98**, 094312 (2005).
- ¹⁴Y. Zhao and R. L. Frost, *J. Raman Spectrosc.* **39**, 1494 (2008).
- ¹⁵M. R. Norman, H. Ding, J. C. Campuzano, T. Takeuchi, M. Randeria, T. Yokoya, T. Takahashi, T. Mochiku, and K. Kadowaki, *Phys. Rev. Lett.* **79**, 3506 (1997).
- ¹⁶T. Valla, A. V. Fedorov, P. D. Johnson, B. O. Wells, S. L. Hulbert, Q. Li, G. D. Gu, and N. Koshizuka, *Science* **285**, 2110 (1999).
- ¹⁷P. Richard, T. Sato, K. Nakayama, S. Souma, T. Takahashi, Y.-M. Xu, G. F. Chen, J. L. Luo, N. L. Wang, and H. Ding, *Phys. Rev. Lett.* **102**, 047003 (2009).
- ¹⁸M. A. Mueller, T. Miller, and T.-C. Chiang, *Phys. Rev. B* **41**, 5214 (1990).
- ¹⁹L. Binet and D. Gourier, *Appl. Phys. Lett.* **77**, 1138 (2000).
- ²⁰T. S. Heng, D.-C. Qi, T. Berlijn, J. B. Yi, K. S. Yang, Y. Dai, Y. P. Feng, I. Santoso, C. Sánchez-Hanke, X. Y. Gao, A. T. S. Wee, W. Ku, J. Ding, and A. Rusydi, *Phys. Rev. Lett.* **105**, 207201 (2010).